Journal of Zhejiang University SCIENCE A
ISSN 1673-565X (Print); ISSN 1862-1775 (Online)
www.zju.edu.cn/jzus; www.springerlink.com
E-mail: jzus@zju.edu.cn

A maximum power point tracker for photovoltaic energy systems based on fuzzy neural networks*

Chun-hua LI†[1], Xin-jian ZHU[1], Guang-yi CAO[1], Wan-qi HU[2], Sheng SUI[1], Ming-ruo HU[1]

([1]*Fuel Cell Research Institute, Shanghai Jiao Tong University, Shanghai 200240, China*)

([2]*Institute of Process Engineering, Chinese Academy of Sciences, Beijing 100080, China*)

†E-mail: viven_lch@163.com

Received Feb. 21, 2008; Revision accepted June 23, 2008; Crosschecked Dec. 26, 2008

Abstract: To extract the maximum power from a photovoltaic (PV) energy system, the real-time maximum power point (MPP) of the PV array must be tracked closely. The non-linear and time-variant characteristics of the PV array and the non-linear and non-minimum phase characteristics of a boost converter make it difficult to track the MPP for traditional control strategies. We propose a fuzzy neural network controller (FNNC), which combines the reasoning capability of fuzzy logical systems and the learning capability of neural networks, to track the MPP. With a derived learning algorithm, the parameters of the FNNC are updated adaptively. A gradient estimator based on a radial basis function neural network is developed to provide the reference information to the FNNC. Simulation results show that the proposed control algorithm provides much better tracking performance compared with the fuzzy logic control algorithm.

Key words: Photovoltaic array, Maximum power point tracking (MPPT), Fuzzy neural network controller (FNNC), Radial basis function neural network (RBFNN)

doi:10.1631/jzus.A0820128 **Document code:** A **CLC number:** TK01; TP2

INTRODUCTION

Due to the scarcity and adverse environmental impacts of conventional fossil fuels, photovoltaic (PV) energy has been attracting more attention in the last few years as a kind of clean and renewable resource. In order to increase the output efficiency of a PV energy system, it is crucial to operate the PV array near the maximum power point (MPP). Generally, a DC-DC converter linking the PV array and the load is used to carry out the maximum power point tracking (MPPT) (Xiao *et al*., 2007a). The boost converter is preferred due to its advantages over the buck converter (Xiao *et al*., 2007b). However, the MPP of the PV array varies with the solar insolation and environmental temperature, as shown in Fig.1. Furthermore, the PV array exhibits extremely non-linear current-voltage characteristic. Its output power depends on the terminal load of the PV system. The non-linear and non-minimum phase characteristics of the boost converter (Shtessel *et al*., 2003) complicate the MPPT further. To overcome these difficulties, some control strategies have been proposed, such as constant voltage (Swiegers and Enslin, 1998), perturb and observe (Santos *et al*., 2006), incremental conductance (Brambilla, 1999), sliding mode (Valenciaga *et al*., 2001), fuzzy logic controller (Patcharaprakiti *et al*., 2005; Altas and Sharaf, 2008), and neural network (Hiyama *et al*., 1995; Torres and Antunes, 1998). However, there still remains a problem of quickly and steadily determining the locus of the MPP when plant parameter variations and external load disturbances occur.

Both the fuzzy logic controller (FLC) and the neural network controller (NNC) have been successfully used in many applications. The fuzzy IF-THEN rules extracted from expert knowledge are used to

* Project (No. 20576071) supported by the National Natural Science Foundation of China

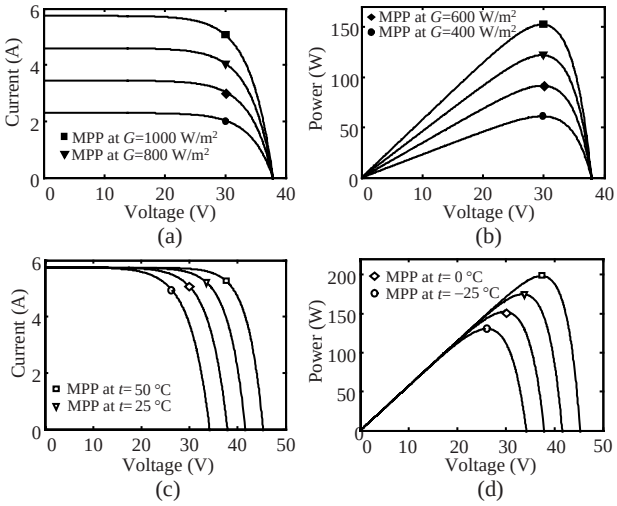

Fig.1 *I-V* and *P-V* characteristic curves of the PV array
(a) *I-V* curves at constant temperature T=298.15 K; (b) *P-V* curves at constant temperature T=298.15 K; (c) *I-V* curves at constant insolation G=1000 W/m^2; (d) *P-V* curves at constant insolation G=1000 W/m^2

express a proper control strategy. Therefore, a precise mathematical model of the plant is not required for the FLC. It is difficult, however, to design the FLC systematically. Furthermore, the static FLC behavior relies significantly on the expert knowledge and has no mechanisms for adapting to the real-time plant change. On the other hand, a neural network possesses the strong ability of learning from the process apart from parallelism and fault tolerance. A learning algorithm is usually used to update the parameters of the network architecture. However, a tremendous amount of training data and a long time are needed to carry out the preliminary off-line learning. It is often difficult to decide the complexity of a structure for the desired control. In addition, the inner workings of the network are invisible to the designer. A fuzzy neural network controller (FNNC) (Lee and Teng, 2000; Lin and Wai, 2002; Lin and Lin, 2004), the combination of an FLC and an NNC, is one of the best controllers to overcome these problems. The NNC provides the connection structure and learning ability to the FLC; the FLC provides a structural framework with the fuzzy IF-THEN rule reasoning to the NNC.

In this study, a four-layer FNNC is designed to track the MPP. The information extracted from the fuzzy control experiences is used to initialize the parameters of the FNNC. An on-line learning algorithm based on the back-propagation method is derived to update the parameters of the FNNC adaptively. In order to provide the reference information to the FNNC, a radial basis function neural network (RBFNN) is used as the gradient estimator. Compared with the traditional FLC, the proposed control approach performs much better.

PHOTOVOLTAIC ENERGY SYSTEM

A schematic overview of the PV energy system is shown in Fig.2. This system consists of a PV array and a boost converter. The dynamic model of the PV energy system can be expressed as (Das *et al*., 2005)

$$\begin{cases} \dfrac{\mathrm{d}v_{\mathrm{pv}}}{\mathrm{d}t} = \dfrac{1}{C_1}(i_{\mathrm{pv}} - i_{L_{\mathrm{c}}}), \\ \dfrac{\mathrm{d}i_{L_{\mathrm{c}}}}{\mathrm{d}t} = \dfrac{1}{L_{\mathrm{c}}}[v_{\mathrm{pv}} - v_{C_2}(1-D)], \\ \dfrac{\mathrm{d}v_{C_2}}{\mathrm{d}t} = \dfrac{1}{C_2}[i_{L_{\mathrm{c}}}(1-D) - v_{C_2}/R_{\mathrm{L}}], \end{cases} \quad (1)$$

where C_1 and C_2 are the input and output capacitors (or capacitance), respectively; L_{c} is the inductor (or inductance); R_{L} and R_{s} are the load and series resistance, respectively; v_{pv} and v_{C_2} are the voltage of the PV array and the voltage of C_2, respectively; i_{pv}, I_{D}, $i_{L_{\mathrm{c}}}$ and i_{L} are the current through PV array, diode D, L_{c}, and the load, respectively; I_{ph} is the photon current.

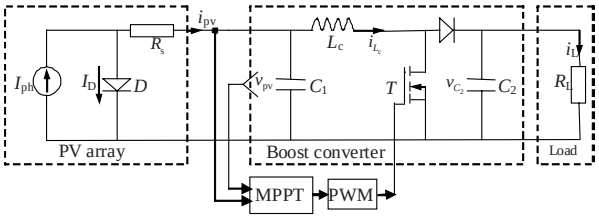

Fig.2 Schematic overview of the PV energy system

Photovoltaic array

As a function of voltage, the current of the PV array is defined by (Xiao *et al*., 2004)

$$i_{\mathrm{pv}} = n_{\mathrm{p}} I_{\mathrm{ph}} - n_{\mathrm{p}} I_{\mathrm{D}} \{\exp[(v_{\mathrm{pv}} + R_{\mathrm{s}} i_{\mathrm{pv}})/(n_{\mathrm{s}} V_{\mathrm{t}})] - 1\}, \quad (2)$$

where n_s is the number of PV cells connected in series, n_p is the number of the cells in parallel, and V_t is the thermal voltage.

The PV array is non-linear and time-variant in nature. The output power of the cells increases with an increase in solar radiation and decreases with an increase in temperature, as shown in Fig.1. There exists a unique MPP on each *P-V* curve. In order to extract the maximum power from the PV array, the MPP must be tracked using an MPP tracker.

Boost converter

The boost converter as shown in Fig.2 is used to track the MPP by tuning its duty ratio D ($0 \le D \le 1$). According to the duty ratio given by the MPPT, a pulse width modulation (PWM) method is used to generate pulse to drive the MOSFET T of the boost converter.

The boost converter is characterized by the non-linearity and non-minimum phase (Shtessel *et al*., 2003). The equivalent resistance of the boost converter can be calculated by (Kazimierczuk and Starman, 1999)

$$R_{eq} = R_L (1-D)^2. \tag{3}$$

According to the power transfer theory, the power delivered to the load is maximized when the equivalent resistance R_{eq} equals the output resistance of the PV array (Mukerjee and Dasgupta, 2007; Zhong *et al*., 2008).

FUZZY NEURAL NETWORK CONTROLLER

The proposed intelligent controller is schematically shown in Fig.3. An adaptive FNNC is adopted as the MPP tracker. The RBFNN-based estimator is designed to provide a reference signal for the FNNC parameter tuning. The condition of an MPP can be described by

$$\frac{\partial P_{pv}}{\partial v_{pv}} = \frac{\partial v_{pv} i_{pv}}{\partial v_{pv}} = v_{pv} \frac{\partial i_{pv}}{\partial v_{pv}} + i_{pv} = 0, \tag{4}$$

where P_{pv} is the output power of the PV array. Hence, the tracking error of the MPP can be calculated as

$$s = \frac{\partial i_{pv}}{\partial v_{pv}} + \frac{i_{pv}}{v_{pv}}. \tag{5}$$

Structure of the FNNC

Fig.4 depicts the FNNC structure, which is a four-layer feedforward connectionist network to realize a simplified fuzzy inference system (Lin and Lin, 2004). The inputs of the FNNC are the tracking error $s(N)$ and the change of the error, $\dot{s}(N)$. The output is the control signal $u(N+1)$ of the PV energy system. Let each input have m membership functions, then the input-output relations between layers are stated as follows:

(1) Layer 1: input layer

$$\begin{cases} I_1^{(1)} = s(N),\ I_2^{(1)} = \dot{s}(N), \\ O_{ij}^{(1)} = k_i(N) I_i^{(1)},\ i = 1, 2;\ j = 1, 2, ..., m, \end{cases} \tag{6}$$

where $\boldsymbol{I}$ is the input vector of the nodes, $\boldsymbol{O}$ is their output vector, k_i is the quantization factor, and N is the number of iterations.

(2) Layer 2: membership layer

In this layer, each node uses a Gaussian function as a membership function.

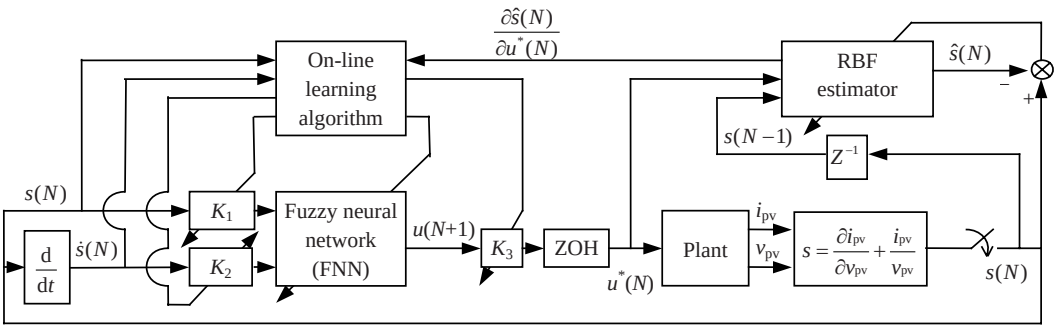

Fig.3 A schematic of the proposed intelligent fuzzy neural network controller

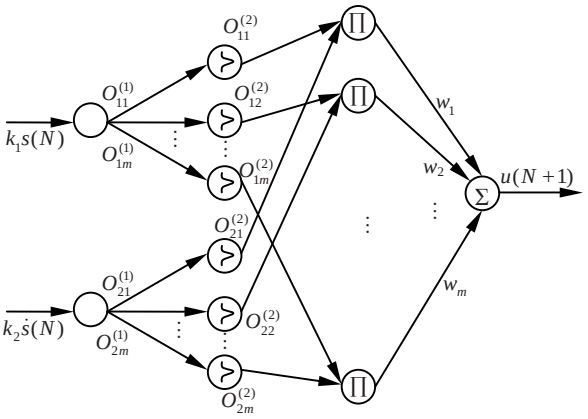

Fig.4 Structure of fuzzy neural network controller

$$\begin{cases} I_{ij}^{(2)} = -\dfrac{(O_{ij}^{(1)} - a_{ij}(N))^2}{(b_{ij}(N))^2}, \\ O_{ij}^{(2)} = \exp(I_{ij}^{(2)}), \end{cases} \tag{7}$$

where a_{ij} and b_{ij} are the center and width of the Gaussian function, respectively.

(3) Layer 3: rule layer

$$\begin{cases} I_l^{(3)} = O_{1l}^{(2)} O_{2l}^{(2)}, \\ O_l^{(3)} = I_l^{(3)}, \end{cases} \quad l = 1, 2, ..., m. \tag{8}$$

(4) Layer 4: output layer

$$\begin{cases} \boldsymbol{I}^{(4)} = \sum_{k=1}^{m} O_k^{(3)} w_k(N), \\ \boldsymbol{O}^{(4)} = u(N+1) = \boldsymbol{I}^{(4)}, \end{cases} \tag{9}$$

where w_k is the connecting weight.

The control input of the plant is defined by

$$u^*(N+1) = k_3(N) \times u(N+1), \tag{10}$$

where k_3 is the scale factor.

On-line learning algorithm

Once an FNNC has been constructed, the learning algorithm aims at determining appropriate values for k_1, k_2, k_3, a_{ij}, b_{ij}, and w_k. Instead of using random numbers, we suggest these parameters be initialized using the expert knowledge from the traditional fuzzy control. These initial settings can generally give more meaningful and stable starting than random initialization. After the initialization process, a gradient-descent-based back-propagation algorithm is employed to adjust the controller parameters.

The energy function is defined as

$$E = \frac{1}{2} k_1(N) \times (s(N))^2. \tag{11}$$

In Layer 4, the error term to be propagated is given by

$$\delta^4 = \frac{\partial E}{\partial s}\frac{\partial s}{\partial u^*} = k_1 s(N) \frac{\partial s(N)}{\partial u^*(N)}. \tag{12}$$

The scale factor and the linking weights are updated by

$$\frac{\partial E}{\partial k_3} = \frac{\partial E}{\partial s}\frac{\partial s}{\partial u^*}\frac{\partial u^*}{\partial k_3} = \delta^4 u(N), \tag{13}$$

$$\frac{\partial E}{\partial w_k} = \frac{\partial E}{\partial s}\frac{\partial s}{\partial u^*}\frac{\partial u^*}{\partial u}\frac{\partial u}{\partial w_k} = \delta^4 k_3(N) O_k^{(3)}. \tag{14}$$

In Layer 2, the error term is computed as

$$\begin{aligned} \delta_{1j}^2 &= \frac{\partial E}{\partial s}\frac{\partial s}{\partial u^*}\frac{\partial u^*}{\partial u}\frac{\partial u}{\partial O_j^{(3)}}\frac{\partial O_j^{(3)}}{\partial O_{1j}^{(2)}}\frac{\partial O_{1j}^{(2)}}{\partial I_{1j}^{(2)}} \\ &= \delta^4 k_3(N) w_l(N) O_{2j}^{(2)} O_{1j}^{(2)} = \delta_{2j}^2. \end{aligned} \tag{15}$$

The centers and the widths of the membership functions are updated by

$$\frac{\partial E}{\partial a_{ij}} = \frac{\partial E}{\partial I_{ij}^{(2)}}\frac{\partial I_{ij}^{(2)}}{\partial a_{ij}} = \delta_{ij}^2 \frac{2(O_{ij}^{(1)} - a_{ij}(N))}{(b_{ij}(N))^2}, \tag{16}$$

$$\frac{\partial E}{\partial b_{ij}} = \frac{\partial E}{\partial I_{ij}^{(2)}}\frac{\partial I_{ij}^{(2)}}{\partial b_{ij}} = \delta_{ij}^2 \frac{2(O_{ij}^{(1)} - a_{ij}(N))^2}{(b_{ij}(N))^3}. \tag{17}$$

The quantization factors are updated by

$$\begin{aligned} \frac{\partial E}{\partial k_i} &= \sum_{j=1}^{m} \frac{\partial E}{\partial I_{ij}^{(2)}}\frac{\partial I_{ij}^{(2)}}{\partial O_{ij}^{(1)}}\frac{\partial O_{ij}^{(1)}}{\partial k_i} \\ &= \sum_{j=1}^{m} \delta_{ij}^2 \frac{-2(O_{ij}^{(1)} - a_{ij}(N))}{(b_{ij}(N))^2} I_i^{(1)}. \end{aligned} \tag{18}$$

Then, the FNNC parameters can be updated by (Lin and Lin, 2004)

$$\begin{cases} w_k(N+1)=w_k(N)-\eta\dfrac{\partial E}{\partial w_k}+\beta\Delta w_k(N), \\ a_{ij}(N+1)=a_{ij}(N)-\eta\dfrac{\partial E}{\partial a_{ij}}+\beta\Delta a_{ij}(N), \\ b_{ij}(N+1)=b_{ij}(N)-\eta\dfrac{\partial E}{\partial b_{ij}}+\beta\Delta b_{ij}(N), \\ k_c(N+1)=k_c(N)-\eta\dfrac{\partial E}{\partial k_c}+\beta\Delta k_c(N),\ c=1,2,3, \end{cases} \tag{19}$$

$$\Delta\chi=\chi(N)-\chi(N-1), \tag{20}$$

where η and β are the leaning rate and the momentum factor, respectively. The only unknown in the proposed learning algorithm is $\dfrac{\partial s(N)}{\partial u^*(N)}$—the gradient of the system output with respect to the control input. Many schemes in the literature can be utilized to evaluate this gradient (Lee and Teng, 2000; Lin and Wai, 2002; Lin and Lin, 2004). In this work, we attempt to develop an on-line gradient estimator based on an RBFNN.

RBFNN-based gradient estimator

A three-layered feedforward RBFNN as shown in Fig.5 is adopted to estimate the gradient $\dfrac{\partial s(N)}{\partial u^*(N)}$. Generally, the RBFNN can uniformly approximate any continuous function to a prospected accuracy. Due to its simple learning algorithm and network structure, the RBFNN possesses a fast-convergence property (Huang *et al*., 2003). Therefore, the RBFNN is adopted to identify the input-output dynamic behavior of the controlled plant and to provide the gradient information to the FNNC. The inputs of the network are the current control input $u^*(N)$ and the most recent output of the plant $s(N-1)$. The output of the network is the estimated value $\hat{s}(N)$ of the tracking error $s(N)$. The signal propagation and the activation function in each layer are introduced as follows:

(1) Input layer

$$\begin{cases} x_1^{(1)}=u^*(N),\ x_2^{(1)}=s(N-1), \\ y_r^{(1)}=x_r^{(1)},\ r=1,2, \end{cases} \tag{21}$$

where $\boldsymbol{x}$ is the input vector of the nodes, and $\boldsymbol{y}$ is their output vector.

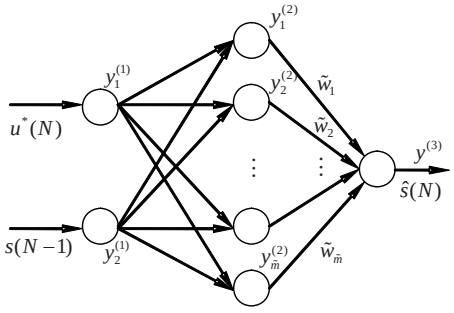

Fig.5 Structure of the three-layer RBFNN-based estimator

(2) Hidden layer

$$\begin{cases} x_v^{(2)}=-\dfrac{(y_1^{(1)}-\phi_{1v}(N))^2+(y_2^{(1)}-\phi_{2v}(N))^2}{2(\sigma_v(N))^2}, \\ y_v^{(2)}=\exp(x_v^{(2)}),\ v=1,2,...,\tilde{m}, \end{cases} \tag{22}$$

where ϕ_{rv} (r=1, 2) and σ_v are the center and width of the Gaussian function, respectively, and $\tilde{m}$ is the number of the hidden-layer nodes.

(3) Output layer

$$\begin{cases} x^{(3)}=\sum_{v=1}^{\tilde{m}}\tilde{w}_v(N)\times y_v^{(2)}, \\ y^{(3)}=\hat{s}(N)=x^{(3)}, \end{cases} \tag{23}$$

where $\tilde{w}_v$ is the connecting weight. The energy function of the RBFNN is defined by

$$e=\frac{1}{2}(s(N)-\hat{s}(N))^2. \tag{24}$$

The parameters ϕ_{rv}, σ_v and $\tilde{w}_v$ can be updated by

$$\begin{cases} \tilde{w}_v(N+1)=\tilde{w}_v(N)-\tilde{\eta}\dfrac{\partial e}{\partial w_v}+\tilde{\beta}\Delta\tilde{w}_v(N), \\ \phi_{rv}(N+1)=\phi_{rv}(N)-\tilde{\eta}\dfrac{\partial e}{\partial \phi_{rv}}+\tilde{\beta}\Delta\phi_{rv}(N), \\ \sigma_v(N+1)=\sigma_v(N)-\tilde{\eta}\dfrac{\partial e}{\partial \sigma_v}+\tilde{\beta}\Delta\sigma_v(N), \end{cases} \tag{25}$$

where $\tilde{\eta}$ and $\tilde{\beta}$ are the learning rate and the momentum factor, respectively. Mean square error *MSE* is employed here to evaluate the identification results,

$$MSE=\frac{1}{N}\sum_{t=1}^{N}(s(t)-\hat{s}(t))^2. \tag{26}$$

By the input-output relationship between $\hat{s}$ and u^* of the RBFNN, we can obtain the required gradient information for the FNNC as follows:

$$\frac{\partial s(N)}{\partial u^*(N)}\approx\frac{\partial\hat{s}(N)}{\partial u^*(N)}=\sum_{v=1}^{\tilde{m}}\frac{\partial\hat{s}}{\partial y^{(3)}}\frac{\partial y^{(3)}}{\partial y_v^{(2)}}\frac{\partial y_v^{(2)}}{x_v^{(2)}}\frac{x_v^{(2)}}{\partial u^*}=\sum_{v=1}^{\tilde{m}}\tilde{w}_v(N)y_v^{(2)}\frac{\phi_{1v}(N)-y_1^{(1)}}{(\sigma_v(N))^2}. \tag{27}$$

SIMULATION

In this section, we implement the proposed control strategy to track the MPP of the PV energy system. A corresponding duty ratio D is given by the FNNC when the changes of the operating conditions occur. According to the duty ratio, the PV energy system is driven to a new MPP by adjusting the equivalent input resistance R_{eq} of the boost converter. As shown in Fig.3, the FNNC is used as the MPP tracker and the RBFNN is used to provide the reference information to the FNNC. A PV array with the surface area of 1.12 m^2 and the highest conversation efficiency of 14% was used in this study. The input capacitance C_1 of the boost converter is 520 μF, its output capacitance C_2 is 420 μF, and its inductance L_c is 76 μH.

Initialization of the controller parameters

Based on the Lyapunov stability approach, rigorous proofs have been presented to guarantee the convergence of the FNNC by choosing appropriate learning rates (Lee and Teng, 2000; Lin and Wai, 2002). In this study, the learning rates are chosen as η=0.18 and β=0.02, which are good enough to obtain satisfactory controlling results. The initial linking weights w_j are listed in Table 1. The other parameters of the FNNC are initialized as follows:

k_1=0.6; k_2=0.6; k_3=1;
[$a_{i1}(0)$, $a_{i2}(0)$, …, $a_{im}(0)$]=[−1, −23/24, …, 23/24, 1];
$b_{ij}(0)$=0.25; i=1, 2; j=1, 2, …, m; m=49.

Some heuristics can be used to roughly initialize the parameters of the RBFNN. Considering the high approximating accuracy and fast convergent speed of the RBFNN, the effect due to the improper selection of the initialized parameters can be retrieved by the on-line updating (Huang *et al*., 2003). Therefore, for simplicity, the parameters of the RBFNN are initialized as follows:

$\tilde{\eta}=0.35;\ \tilde{\beta}=0.05;\ \tilde{w}_v=0;\ \phi_{rv}=0.1;\ \sigma_v=3;$
$r=1,\ 2;\ v=1, 2, ..., \tilde{m};\ \tilde{m}=4.$

Table 1 The initial linking weights of the FNNC

$\dot{s}$	Initial linking weight						
	s=NB	NM	NS	ZO	PS	PM	PB
NB	1 (w_1)	1 (w_8)	2/3	2/3	1/3	1/3	0 (w_{43})
NM	1 (w_2)	2/3	2/3	1/3	1/3	0	−1/3
NS	2/3	2/3	1/3	1/3	0	−1/3	−1/3
ZO	2/3	1/3	1/3	0	−1/3	−1/3	−2/3
PS	1/3	1/3	0	−1/3	−1/3	−2/3	−2/3
PM	1/3	0	−1/3	−1/3	−2/3	−2/3	−1 (w_{48})
PB	0 (w_7)	−1/3	−1/3	−2/3	−2/3	−1 (w_{42})	−1 (w_{49})

s: experimental MPP tracking error; $\dot{s}$: the change of s. NB: negative big; NM: negative middle; NS: negative small; ZO: zero; PS: positive small; PM: positive middle; PB: positive big

Results and discussion

In order to show the effectiveness of the proposed control algorithm, a traditional FLC is also used to track the MPP (Patcharaprakiti *et al*., 2005). The atmospheric conditions (insolation and temperature) and load disturbance are shown in Fig.6. The quantization factors k_1, k_2 and scale factor k_3 are adaptive to condition variations, as shown in Fig.7. The comparison between the experimental error s and the error $\hat{s}$ acquired by the RBFNN is shown in Fig.8. The *MSE* of the error s is 0.0041. This approximating accuracy is acceptable for the control purpose. Figs.9a~9c depict the output voltage, current, and power of the PV array regulated by the MPPT, respectively. By incorporating the expert knowledge into the neural network, the convergence speed and stability of the FNNC are improved, especially in the first cycle of periodic step-commands. The traditional FLC needs 10 ms to reach the stable state and its overshoot is big. The reason is that the initial setting of the FLC is unsuitable and cannot be updated on-line. Comparatively, the proposed algorithm is much better than the traditional FLC, and it needs only not more than 2 ms with small overshoots and oscillations to reach the steady state.

The errors of the MPPT for the FLC and the proposed FNNC are shown in Fig.10. Although both control algorithms can acquire the MPP under variant operating conditions, in the proposed FNNC the tracking error s converges to zero more quickly and steadily.

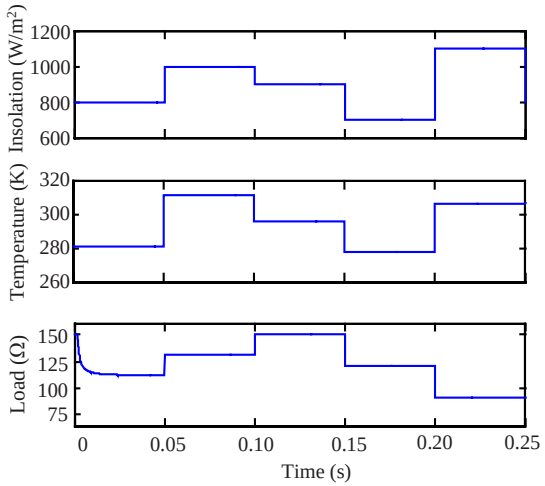

Fig.6 Atmospheric conditions (insolation and temperature) and load disturbance of the PV system

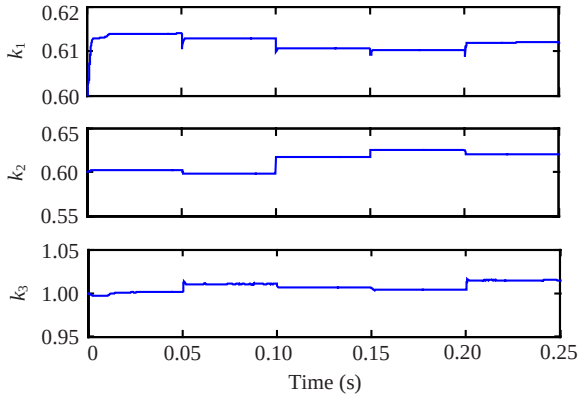

Fig.7 Changes of quantization factors (k_1, k_2) and scale factor (k_3) under variant operating conditions

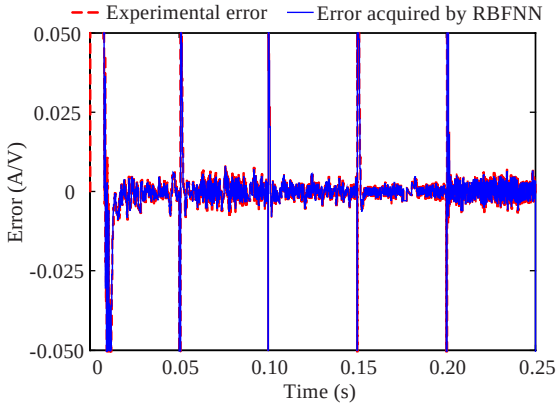

Fig.8 Comparison between the experimental error s and the error $\hat{s}$ acquired by the RBFNN

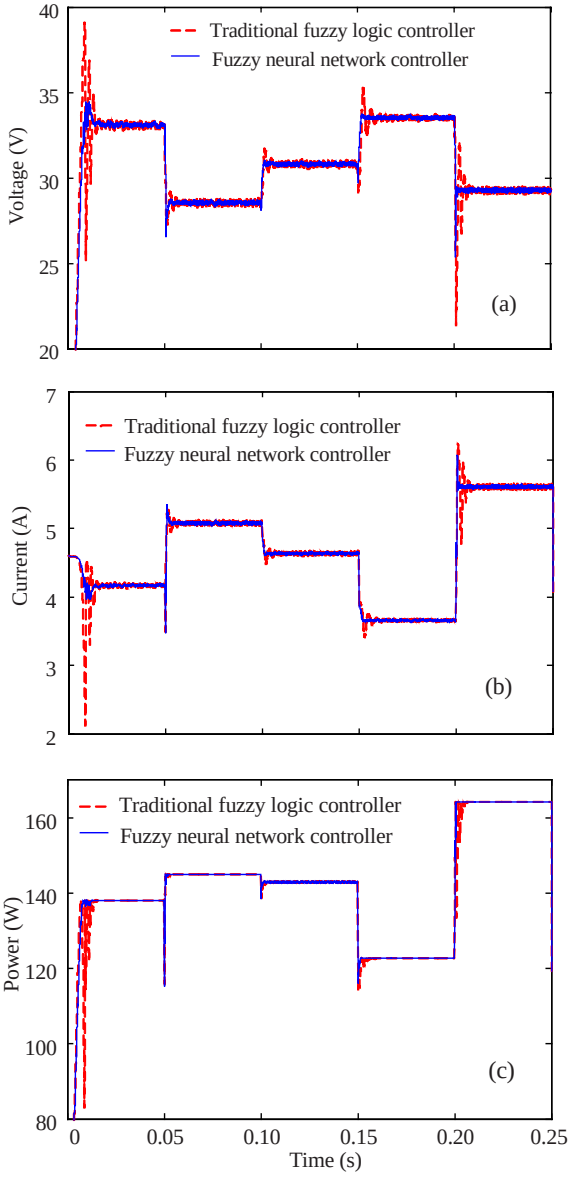

Fig.9 Regulated output voltage (a), current (b), and power (c) of the PV energy system

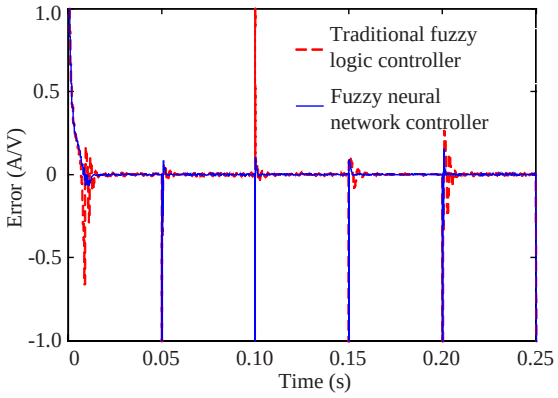

Fig.10 Error of MPPT for the PV energy system

CONCLUSION

In this paper, an intelligent control strategy has been proposed for the MPPT of a PV energy system. A four-layer FNNC is adopted as the process feedback controller. The FNNC is initialized using the expert knowledge from the traditional fuzzy control, which alleviates the burden of the lengthy pre-learning. With a derived learning algorithm, the parameters in the FNNC are updated adaptively by observing the tracking error. An RBFNN is designed to provide the FNNC with the gradient information, which avoids the complexity of the PV energy system. The experimental results show that the FNNC tracks the MPP quickly and steadily, exhibits good robustness to the parameter variants and external load disturbances, and performs much better compared with the traditional FLC.

References

Altas, I.H., Sharaf, A.M., 2008. A novel maximum power fuzzy logic controller for photovoltaic solar energy systems. *Renewable Energy*, **33**(3):388-399. [doi:10.1016/j.renene.2007.03.002]

Brambilla, A., 1999. New Approach to Photovoltaic Arrays Maximum Power Point Tracking. 30th Annual IEEE Power Electronics Specialists Conf., South Carolina, USA, p.632-637.

Das, D., Esmaili, R., Xu, L., Nichols, D., 2005. An Optimal Design of a Grid Connected Hybrid Wind/Photovoltaic/Fuel Cell System for Distributed Energy Production. 32nd Annual Conf. of the IEEE Industrial Electronics Society, Paris, France, p.2499-2504.

Hiyama, T., Kouzuma, S., Imakubo, T., Ortmeyer, T.H., 1995. Evaluation of neural network based real time maximum power tracking controller for PV system. *IEEE Trans. Energy Conv.*, **10**(3):543-548. [doi:10.1109/60.464880]

Huang, S.J., Huang, K.S., Chiou, K.C., 2003. Development and application of a novel radial basis function sliding mode controller. *Mechatronics*, **13**(4):313-329. [doi:10.1016/S0957-4158(01)00050-2]

Kazimierczuk, M.K., Starman, L.A., 1999. Dynamic performance of PWM DC-DC boost converter with input voltage feedforward control. *IEEE Trans. Circuits Syst. I: Fundam. Theory Appl.*, **46**(12):1473-1481. [doi:10.1109/81.809549]

Lee, C.H., Teng, C.C., 2000. Identification and control of dynamic systems using recurrent fuzzy neural networks. *IEEE Trans. Fuzzy Syst.*, **8**(4):349-366. [doi:10.1109/91.868943]

Lin, F.J., Lin, C.H., 2004. A permanent-magnet synchronous motor servo drive using self-constructing fuzzy neural network controller. *IEEE Trans. Energy Conv.*, **19**(1):66-72. [doi:10.1109/TEC.2003.821835]

Lin, F.J., Wai, R.J., 2002. Adaptive fuzzy-neural-network control for induction spindle motor drive. *IEEE Tran. Energy Conv.*, **17**(4):507-513. [doi:10.1109/TEC.2002.805225]

Mukerjee, A.K., Dasgupta, N., 2007. DC power supply used as photovoltaic simulator for testing MPPT algorithms. *Renewable Energy*, **32**(4):587-592. [doi:10.1016/j.renene.2006.02.010]

Patcharaprakiti, N., Premrudeepreechacharn, S., Sriuthaisiriwong, Y., 2005. Maximum power point tracking using adaptive fuzzy logic control for grid-connected photovoltaic system. *Renewable Energy*, **30**(11):1771-1788. [doi:10.1016/j.renene.2004.11.018]

Santos, J.L., Antunes, F., Chehab, A., Cruz, C., 2006. A maximum power point tracker for PV systems using a high performance boost converter. *Solar Energy*, **80**(7):772-778. [doi:10.1016/j.solener.2005.06.014]

Shtessel, Y.B., Zinober, A.S.I., Shkolnikov, I.A., 2003. Sliding mode control of boost and buck-boost power converters using method of stable system centre. *Automatica*, **39**(6):1061-1067. [doi:10.1016/S0005-1098(03)00068-2]

Swiegers, W., Enslin, J.H.R., 1998. An Integrated Maximum Power Point Tracker for Photovoltaic Panels. Proc. IEEE Int. Symp. on Industrial Electronics, Pretoria, South Africa, p.40-44.

Torres, A.M., Antunes, F.L.M., 1998. An Artificial Neural Network-based Real Time Maximum Power Tracking Controller for Connecting a PV System to the Grid. 24th Annual Conf. of the IEEE Industrial Electronics Society, Aachen, Germany, p.554-558.

Valenciaga, F., Puleston, P.F., Battaiotto, P.E., 2001. Power control of a photovoltaic array in a hybrid electric generation system using sliding mode techniques. *IEE Proc.-Control Theory Appl.*, **148**(6):448-455. [doi:10.1049/ip-cta:20010785]

Xiao, W., Dunford, W.G., Capel, A., 2004. A Novel Modeling Method for Photovoltaic Cells. IEEE Power Electronics Specialists Conf., Aachen, Germany, p.1950-1956.

Xiao, W., Dunford, W.G., Palmer, P.R., Capel, A., 2007a. Regulation of photovoltaic voltage. *IEEE Trans. Ind. Electron.*, **54**(3):1365-1374. [doi:10.1109/TIE.2007.893059]

Xiao, W., Ozog, N., Dunford, W.G., 2007b. Topology study of photovoltaic interface for maximum power point tracking. *IEEE Trans. Ind. Electron.*, **54**(3):1696-1704. [doi:10.1109/TIE.2007.894732]

Zhong, Z.D., Huo, H.B., Zhu, X.J., 2008. Adaptive maximum power point tracking control of fuel cell power plants. *J. Power Sources*, **176**:259-269. [doi:10.1016/j.jpowsour.2007.10.080]